Calculation of Pulsar Microstructure Using Quantum Gravity Theory with Ultimate Acceleration

Huaiyang Cui
Department of Physics, Beihang University, Beijing, 102206, China
Email: hycui@buaa.edu.cn
(October 12, 2022, submitted to viXra)

Abstract: In analogy with the ultimate speed c, there is an ultimate acceleration β, nobody's acceleration can exceed this limit β, in the solar system, β=2.961520e+10(m/s^2). Because this ultimate acceleration is large, any effect related to β will become easy to test, including quantum gravity tests. In this paper, an approach is put forward to connect the ultimate acceleration with quantum theory, as an application, the sunspot cycle is calculated to be 10.38 years due to the ultimate acceleration. The same approach is applied to pulsar microstructure problems. The microstructures of pulsar PSR J0437-4715 at 436Mhz and PSR B0950+08 at 430Mhz are investigated, the calculation results agree well with the observations. Under non-relativistic condition, the pulsar with 100 times solar mass has a period of 2.09s; the pulsar with 10 solar times mass has a period of 0.2s; the pulsar with solar mass has a period of 20ms; the pulsar with a tenth solar mass has a period of 2ms.

1. Introduction

In general, some quantum gravity proposals [1,2] are extremely hard to test in practice, as quantum gravitational effects are appreciable only at the Planck scale [3]. But ultimate acceleration provides another scheme to deal with quantum gravity effects.

In analogy with the ultimate speed c, there is an ultimate acceleration β, nobody's acceleration can exceed this limit β, in the solar system, β=2.961520e+10(m/s^2). Because this ultimate acceleration is large, any effect related to β will become easy to test, including quantum gravity tests. In this paper, an approach is put forward to connect the ultimate acceleration with quantum theory, as an application, the sunspot cycle is calculated to be 10.38 years due to the ultimate acceleration. The same approach is applied to pulsar microstructure problems.

2. How to connect the ultimate acceleration with quantum theory

In relativity, the speed of light c is the ultimate speed, nobody's speed can exceed this limit c. The relativistic velocity u of a particle in the coordinate system ($x_1,x_2,x_3,x_4=ict$) satisfies

$$u_1^2+u_2^2+u_3^2+u_4^2=-c^2 \quad . \tag{1}$$

No matter what particles (electrons, molecules, neutrons, quarks), their 4-vector velocities all have the same magnitude: $|u|=ic$. All particles gain **equality** because of the same magnitude of the 4-velocity u. The acceleration a of a particle is given by

$$a_1^2 + a_2^2 + a_3^2 = a^2; \quad (a_4 = 0; \quad \because x_4 = ict) \tag{2}$$

Assume that particles have an ultimate acceleration β as the limit, no particle can exceed this acceleration limit β. Subtracting both sides of the above equation by β^2, we have

$$a_1^2 + a_2^2 + a_3^2 - \beta^2 = a^2 - \beta^2; \qquad a_4 = 0 \tag{3}$$

It can be rewritten as

$$[a_1{}^2 + a_2{}^2 + a_3{}^2 + 0 + (i\beta)^2]\frac{1}{1 - a^2/\beta^2} = -\beta^2 \tag{4}$$

Now, the particle has an acceleration whose five components are specified by

$$\begin{aligned} &\alpha_1 = \frac{a_1}{\sqrt{1-a^2/\beta^2}}; \quad \alpha_2 = \frac{a_2}{\sqrt{1-a^2/\beta^2}}; \\ &\alpha_3 = \frac{a_3}{\sqrt{1-a^2/\beta^2}}; \quad \alpha_4 = 0; \quad \alpha_5 = \frac{i\beta}{\sqrt{1-a^2/\beta^2}}; \end{aligned} \tag{5}$$

where α_5 is the newly defined acceleration in five-dimensional space-time ($x_1, x_2, x_3, x_4 = ict, x_5$). Thus, we have

$$\alpha_1^2 + \alpha_2^2 + \alpha_3^2 + \alpha_4^2 + \alpha_5^2 = -\beta^2; \quad \alpha_4 = 0 \tag{6}$$

It means that the magnitude of the newly defined acceleration α for every particle takes the same value: $|\alpha| = i\beta$ (constant imaginary number), all particle accelerations gain **equality** for the sake of the same magnitude.

How do resolve the velocity u and acceleration α into x, y, and z components? In a realistic world, a hand can rotate a ball moving around a circular path at constant speed v with constant centripetal acceleration a, as shown in Fig.1(a). Likewise, the u and α let the particle move spirally, as shown in Fig.1(b), projecting out the real x, y, and z components.

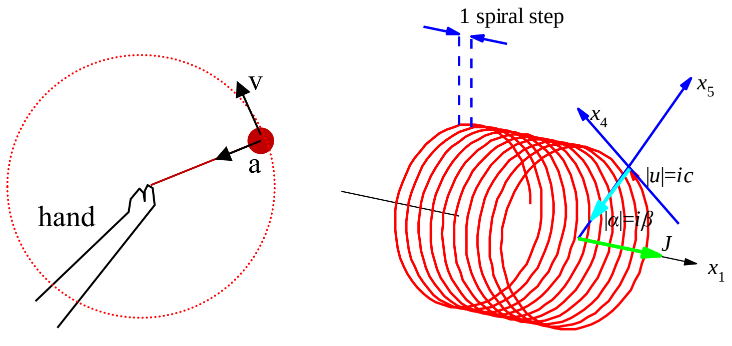

(a) (b) right hand chirality

Fig.1 (a) A hand rotates a ball moving around a circular path at constant speed v with constant centripetal acceleration a. (b) The particle moves along the x_1 axis with the constant speed $|u|=ic$ in u direction and constant centripetal force in the x_5 axis at the radius iR (imaginary number).

```
<Clet2020 Script>//[26]
double D[100],S[2000];int i,j,R,X,N;
int main(){R=50;X=50;N=600;D[0]=-50;D[1]=0;D[2]=0;D[3]=X;D[4]=0;D[5]=0;D[6]=-50;D[7]=R;D[8]=0;
D[9]=600;D[10]=10;D[11]=R;D[12]=0;D[13]=3645;
Lattice(SPIRAL,D,S);SetViewAngle(0,80,-50);DrawFrame(FRAME_NULL,1,0xffffff);
Draw("LINE,0,2,XYZ,0","-150,0,0,-50,0,0");Draw("ARROW,0,2,XYZ,10","50,0,0,150,0,0");
SetPen(2,0xff0000);Plot("POLYLINE,0,600,XYZ",S[9]);i=9+3*N-6;Draw("ARROW,0,2,XYZ,10",S[i]);
TextHang(S[i],S[i+1],S[i+2],"   #if|u|=ic#t");TextHang(150,0,0,"   #ifx#sd1#t");SetPen(2,0x005fff);
Draw("LINE,1,2,XYZ,8","-50,0,50,-50,0,100");Draw("LINE,1,2,XYZ,8","-40,0,50,-40,0,100");
```

```
Draw("ARROW,0,2,XYZ,10","-80,0,100,-50,0,100");Draw("ARROW,0,2,XYZ,10","-10,0,100,-40,0,100");
TextHang(-50,0,110,"1 spiral step");i=9+3*N;S[i]=50;S[i+1]=10;S[i+2]=10;
Draw("ARROW,0,2,XYZ,10","50,0,0,50,80,80");TextHang(50,80,80," #ifx#sd5#t");
Draw("ARROW,0,2,XYZ,10","50,72,0,50,0,72");TextHang(50,0,72,"   #ifx#sd4#t");
SetPen(3,0x00ffff);Draw("ARROW,0,2,XYZ,15",S[i-3]);TextHang(S[i],S[i+1],S[i+2],"   #if|α|=iβ#t");
SetPen(3,0x00ff00);Draw("ARROW,0,2,XYZ,15","50,0,0,120,0,0");TextHang(110,5,5," #ifJ#t");
TextHang(-60,0,-80," right hand chirality");}#v07=?>A#t
```

In analogy with the ball in a circular path, consider a particle in one-dimensional motion along the x_1 axis at the speed v, in Fig.1(b) it moves with the constant speed $|u|=ic$ almost along the x_4 axis and slightly along the x_1 axis, and the constant centripetal acceleration $|\alpha|=i\beta$ in the x_5 axis at the constant radius iR (imaginary number); the coordinate system ($x_1,x_4=ict,x_5=iR$) establishes a cylinder coordinate system in which this particle moves spirally at the speed v along the x_1 axis. According to the usual centripetal acceleration formula $a=v^2/r$, the acceleration in the x_4-x_5 plane is given by

$$a=\frac{v^2}{r} \quad \Rightarrow \quad i\beta=\frac{|u|^2}{iR}=-\frac{c^2}{iR}=i\frac{c^2}{R} \quad . \tag{7}$$

Therefore, the track of the particle in the cylinder coordinate system ($x_1,x_4=ict,x_5=iR$) forms a shape, called **acceleration-roll**. The faster the particle moves along the x_1 axis, the longer the spiral step is.

Like a steel spring that contains an elastic wave, the track in the acceleration-roll in Fig.1(b) can be described by a wave function whose phase changes 2π for one spiral step. Apparently, this wave is just the de Broglie's matter wave for electrons, protons or quarks, etc.

Theorem: the acceleration-roll bears matter wave.

$$\psi=\exp\left(i\frac{\beta}{c^3}\int_0^x (u_1dx_1+u_2dx_2+u_3dx_3+u_4dx_4)\right) \quad . \tag{8}$$

Proof: See ref. [28,30].

Depending on the particle under investigation, this wave function may have different explanations. If the β is replaced by the Planck constant, the wave function of electrons is given by

$$\begin{aligned} &assume: \quad \beta=\frac{mc^3}{\hbar} \\ &\psi=\exp\left(\frac{i}{\hbar}\int_0^x (mu_1dx_1+mu_2dx_2+mu_3dx_3+mu_4dx_4)\right) \end{aligned} \quad . \tag{9}$$

where $mu_4dx_4=-Edt$, it strongly suggests that the wave function is just the de Broglie's matter wave [4,5,6].

Considering another explanation to ψ for planets in the solar system, no Planck constant can be involved. But, in a many-body system with the total mass M, the data analysis [28] tells us that the ultimate acceleration can be rewritten in terms of **Planck-constant-like constant** h as

$$
\begin{aligned}
&assume: \quad \beta = \frac{c^3}{hM} \\
&\psi = \exp\left(\frac{i}{hM}\int_0^x (u_1 dx_1 + u_2 dx_2 + u_3 dx_3 + u_4 dx_4)\right)
\end{aligned} \qquad (10)
$$

The constant h will be determined by experimental observations. This paper will show that this wave function is applicable to several many-body systems in the solar system, the wave function is called the **acceleration-roll wave**.

Tip: actually, ones cannot get to see the acceleration-roll of a particle in the relativistic space-time ($x_1,x_2,x_3,x_4=ict$) ; only get to see it in the cylinder coordinate system ($x_1,x_4=ict,x_5=iR$).

3. How to determine the ultimate acceleration

In Bohr's orbit model for planets or satellites, as shown in Fig.2, the circular quantization condition is given in terms of relativistic matter wave in gravity by

$$
\left.\begin{aligned}
&\frac{\beta}{c^3}\oint_L v_l dl = 2\pi n \\
&v_l = \sqrt{\frac{GM}{r}}
\end{aligned}\right\} \Rightarrow \quad \sqrt{r} = \frac{c^3}{\beta\sqrt{GM}} n; \quad n = 0,1,2,\ldots \qquad (11)
$$

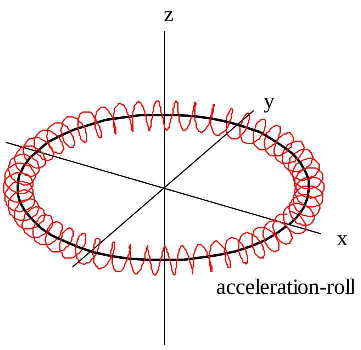

Fig.2 A planet 2D orbit around the sun, an acceleration-roll winding around the planet.

```
<Clet2020 Script>//[26]
int i,j,k; double r,rot,x,y,z,D[20],F[20],S[200]; int main(){SetViewAngle("temp0,theta60,phi-30");
DrawFrame(FRAME_LINE,1,0xafffaf);r=80;Spiral(); TextHang(r,-r,0,"acceleration-roll");
r=110;TextHang(r,0,0,"x");TextHang(0,r,0,"y");TextHang(0,0,r,"z");}
Spiral(){r=80;j=10;rot=j/r;k=2*PI/rot+1;
for(i=0;i<k;i+=1) {D[0]=x;D[1]=y;D[2]=z;D[6]=x;D[7]=y;D[8]=r;
x=r*cos(rot*i);y=r*sin(rot*i);z=0;if(i==0) continue;
SetPen(2,0x00);F[0]=D[0];F[1]=D[1];F[2]=x;F[3]=y;Draw("LINE,0,2,XY,",F);SetPen(1,0xff0000);
D[3]=x;D[4]=y;D[5]=z; D[9]=40;D[10]=10;D[11]=8;D[12]=0;D[13]=360;
Lattice(SPIRAL,D,S);Plot("POLYLINE,0,40,XYZ",S[9]);}
}#v07=?>A#t
```

The solar system, Jupiter's satellites, Saturn's satellites, Uranus' satellites, and Neptune's satellites as five different many-body systems are investigated with the Bohr's orbit model. After fitting observational data as shown in Fig.3, their ultimate accelerations are obtained in Table 1. The predicted quantization blue-lines in Fig.3(a), Fig.3(b), Fig.3(c), Fig.3(d) and Fig.3(e) agree well with experimental observations for those *inner constituent planets or satellites*.

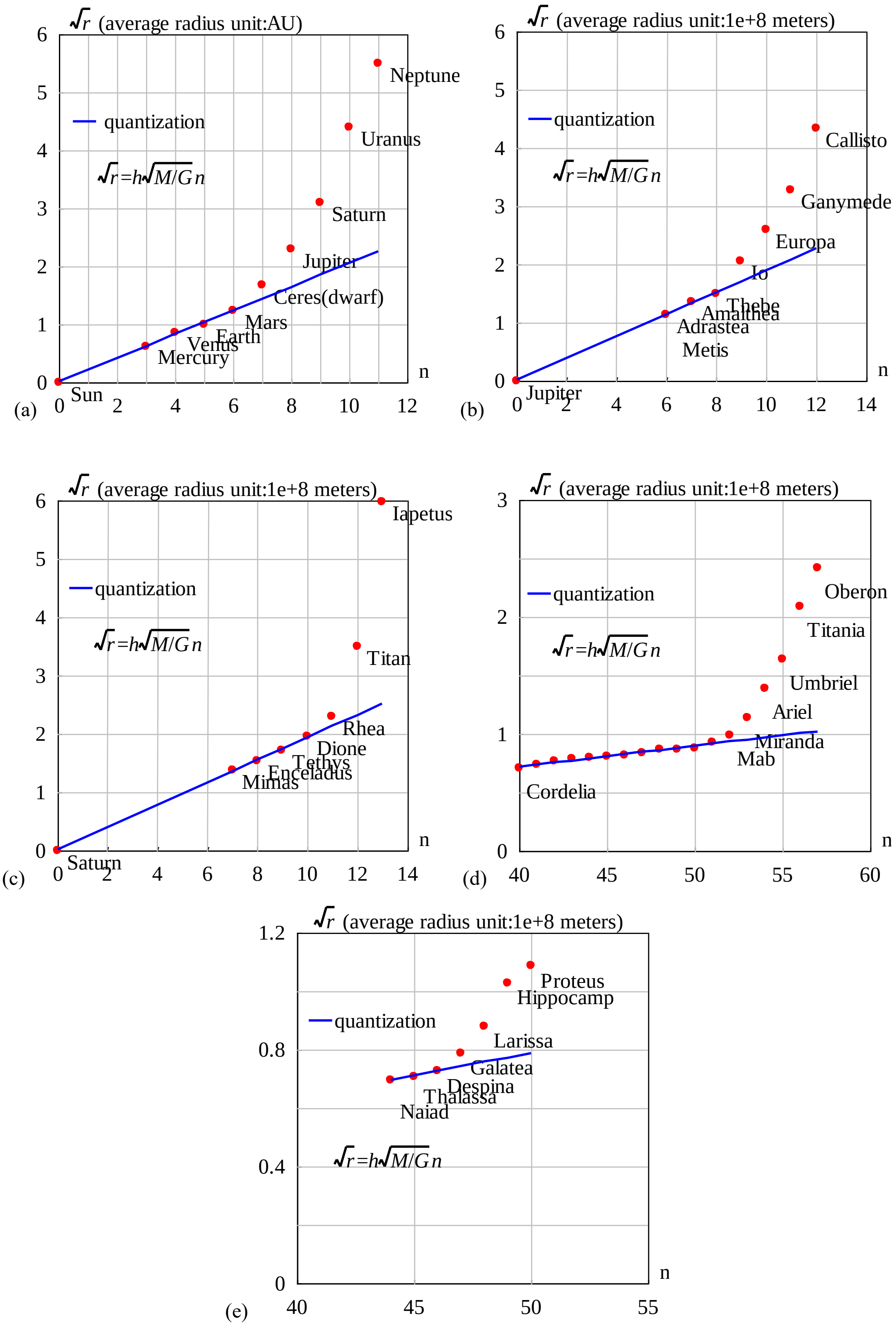

Fig.3 The orbital radii are quantized for inner constituents. (a) the solar system with h=4.574635e-16 ($m^2s^{-1}kg^{-1}$). The relative error is less than 3.9%. (b) the Jupiter system with h=3.531903e-16 ($m^2s^{-1}kg^{-1}$). Metis and Adrastea are assigned the same quantum number for their almost same radius. The relative error is less than 1.9%. (c) the Saturn system with h=6.610920e-16 ($m^2s^{-1}kg^{-1}$). The relative error is less than 1.1%. (d) the Uranus system with h=1.567124e-16 ($m^2s^{-1}kg^{-1}$). n=0 is assigned to Uranus. The relative error is less than 2.5%. (e) the Neptune system with h=1.277170e-16 ($m^2s^{-1}kg^{-1}$). n=0 is assigned to Neptune. The relative error is less than 0.17%.

Table 1 Planck-constant-like constant h, N is constituent particle number with smaller orbital inclination.

system	N	M/M_{earth}	β (m/s2)	h (m2s-1kg-1)	Prediction
Solar planets	9	333000	2.961520e+10	4.574635e-16	Fig.3(a)
Jupiter' satellites	7	318	4.016793e+13	3.531903e-16	Fig.3(b)
Saturn's satellites	7	95	7.183397e+13	6.610920e-16	Fig.3(c)
Uranus' satellites	18	14.5	1.985382e+15	1.567124e-16	Fig.3(d)
Neptune 's satellites	7	17	2.077868e+15	1.277170e-16	Fig.3(e)

Besides every β, our interest shifts to the constant h in Table 1, which is defined as

$$h = \frac{c^3}{M\beta} \quad \Rightarrow \quad \sqrt{r} = h\sqrt{\frac{M}{G}}n \ . \tag{12}$$

In a many-body system with a total mass of M, a constituent particle has the mass of m and moves at the speed of v, it is easy to find that the wavelength of de Broglie's matter wave should be modified for planets and satellites as

$$\lambda_{de\_Broglie} = \frac{2\pi\hbar}{mv} \quad \Rightarrow \text{modify} \Rightarrow \quad \lambda = \frac{2\pi hM}{v} \ . \tag{13}$$

where h is a **Planck-constant-like constant**. Usually, the total mass M is approximately equal to the central-star's mass. It is found that this modified matter wave works for quantizing orbits correctly in Fig.3 [28,29]. The key point is that the various systems have almost the same Planck-constant-like constant h in Table 1 with a mean value of 3.51e-16 $m^2s^{-1}kg^{-1}$, at least having the same magnitude! The acceleration-roll wave is a generalized matter wave on a planetary scale.

In Fig.3(a), the blue straight line expresses the linear regression relation among the Sun, Mercury, Venus, Earth and Mars, their quantization parameters are hM=9.098031e+14(m^2/s). The ultimate acceleration is fitted out to be β=2.961520e+10 (m/s^2). Where, n=3,4,5,.. were assigned to solar planets, the sun was assigned a quantum number n=0 because the sun is in the **central state**.

4. Optical model of the central state

The acceleration-roll wave as the relativistic matter wave generalized in gravity is given by

$$\psi = \exp\left(\frac{i}{hM}\int_0^x v_l dl\right); \quad \lambda = \frac{2\pi hM}{v_l} = \frac{2\pi c^3}{v_l\beta} \ . \tag{14}$$

In a central state n=0, if the coherent length of the acceleration-roll wave is long enough, its head may overlap with its tail when the particle moves in a closed orbit in space-time, as shown in Fig.4, the interference of the acceleration-roll wave between its head and tail will occur in the overlapping zone. The overlapped wave is given by

$$\psi(r) = 1 + e^{i\delta} + e^{i2\delta} + ... + e^{i(N-1)\delta} = \frac{1-\exp(iN\delta)}{1-\exp(i\delta)}$$
$$\delta(r) = \frac{1}{hM}\oint_L (v_l)dl = \frac{2\pi\omega r^2}{hM} = \frac{2\pi\beta\omega r^2}{c^3} \quad . \tag{15}$$

where N is the overlapping number which is determined by the coherent length of the acceleration-roll wave, δ is the phase difference after one orbital motion, ω is the angular speed of the solar rotation. The above equation is a multi-slit interference formula in optics, for a larger N it is called the Fabry-Perot interference formula.

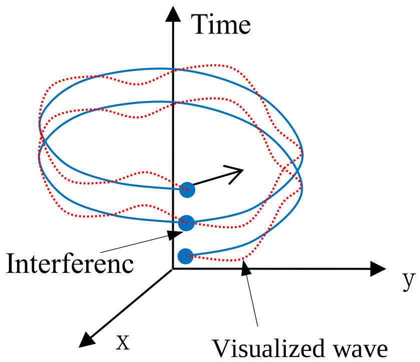

Fig.4 The head of the acceleration-roll wave may overlap with its tail.

The acceleration-roll wave function ψ needs a further explanation. In quantum mechanics, $|\psi|^2$ equals to the probability of finding an electron due to Max Burn's explanation; in astrophysics, $|\psi|^2$ equals to the probability of finding a nucleon (proton or neutron) *averagely on an astronomic scale*, because all mass is mainly made of nucleons, we have

$$|\psi|^2 \propto nucleon\_density \quad . \tag{16}$$

It follows from the multi-slit interference formula that the interference intensity at maxima is proportional to N^2, that is

$$N^2 = \frac{|\psi(0)_{multi-wavelet}|^2}{|\psi(0)_{one-wavelet}|^2} \quad . \tag{17}$$

What matter plays the role of "one-wavelet" in the solar core or earth core? We choose air-vapor at the sea level on the earth's surface as the "reference matter: one-wavelet". Thus, the overlapping number N is estimated by

$$N^2 = \frac{|\psi(0)_{multi-wavelet}|^2}{|\psi(0)_{one-wavelet}|^2} \approx \frac{core\_nucleon\_density_{r=0}}{air\_vapor\_density_{r=sea}} \quad . \tag{18}$$

Although today there is no air-vapor on the solar surface, does not hinder to select it as the reference matter. The solar core has a maximum density of 1.5e+5kg/m^3 [31], comparing to the air-vapor density of 1.29 kg/m^3 at the sea level on the earth, the solar overlapping number N is estimated as N=341. The earth's core density is 5.53e+3kg/m^3, the earth's overlapping number N is estimated as N=65.

For the Sun, Earth and Mars, their central densities and their reference matter density are given in Table 2. Thus, their overlapping numbers are estimated also in this table.

Sun's angular speed at the equator is known as $\omega=2\pi/(25.05*24*3600)$, unit: s^{-1}. Its mass 1.9891e+30 (kg), radius 6.95e+8 (m), mean density 1408 (kg/m^3), the solar core has a maximum density of 1.5e+5kg/m^3 [31], the ultimate acceleration β=2.961520e+10 (m/s^2), the constant hM= 9.100745e+14 (m^2/s). According to the N=341, the matter distribution of the $|\psi|^2$ is calculated in Fig.5, it agrees well with the general description of the sun's interior. The radius of the sun is calculated to be r=7e+8 (m) with a relative error of 0.72% in Fig.5, which indicates that the sun radius strongly depends on the sun's self-rotation.

Table 2 Estimating the overlapping number N by comparing solid core to reference matter, regarding protons and neutrons as basis particles.

object	Solid core, density (kg/m^3)	Reference matter, density (kg/m^3)	Overlapping number N	β (m/s^2)
Sun	1.5e+5 (max.)	1.29 (vapor above the sea)	341	2.961520e+10
Earth	5530	1.29 (vapor above the sea)	65	1.377075e+14
Mars	3933.5	1.29 (vapor above the sea)	55	2.581555e+15
Jupiter	1326			4.016793e+13
Saturn	687			7.183397e+13
Uranus	1270			1.985382e+15
Neptune	1638			2.077868e+15
Alien-planet	5500	1.29(has water on the surface)	65	

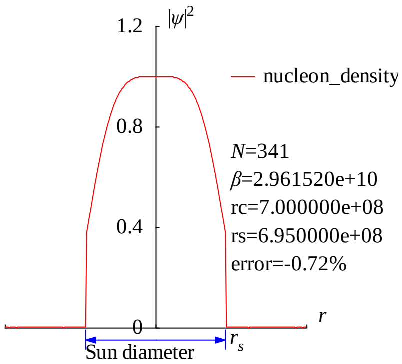

Fig.5 The matter distribution $|\psi|2$ around the Sun has been calculated in the radius direction.

```
<Clet2020 Script>//[26]
int i,j,k,m,n,N,nP[10];
double beta,H,B,M,r,r_unit,x,y,z,delta,D[1000],S[1000], a,b,rs,rc,rot,atm_height; char str[100];
main(){k=150;rs=6.95e8;rc=0;x=25.05;rot=2*PI/(x*24*3600);n=0; N=341;
beta=2.961520e10;H=SPEEDC*SPEEDC*SPEEDC/beta;M=1.9891E30; atm_height=2e6; r_unit=1E7;
b=PI/(2*PI*rot*rs*rs/H);
for(i=-k;i<k;i+=1) {r=abs(i)*r_unit;
if(r<rs+atm_height) delta=2*PI*rot*r*r/H; else delta=2*PI*sqrt(GRAVITYC*M*r)/H;//around the star
y=SumJob("SLIT_ADD,@N,@delta",D); y=y/(N*N);
S[n]=i;S[n+1]=y; if(i>0 && rc==0 && y<0.001) rc=r;D[n]=i;D[n+1]=z;n+=2;}
SetAxis(X_AXIS,-k,0,k,"#ifr; ; ; ;");SetAxis(Y_AXIS,0,0,1.2,"#if|ψ|#su2#t;0;0.4;0.8;1.2;");
DrawFrame(FRAME_SCALE,1,0xafffaf); z=100*(rs-rc)/rs;
SetPen(1,0xff0000);Polyline(k+k,S,k/2,1," nucleon_density"); SetPen(1,0x0000ff); //Polyline(k+k,D);
//Draw("LINE,0,2,XY,0","20,0.5,60,0.6");TextHang(60,0.6,0,"core");
r=rs/r_unit;y=-0.05;D[0]=-r;D[1]=y;D[2]=r;D[3]=y; Draw("ARROW,3,2,XY,10,100,10,10,",D);
Format(str,"#ifN#t=%d#n#ifβ#t=%e#nrc=%e#nrs=%e#nerror=%.2f%",N,beta,rc,rs,z);
TextHang(k/2,0.7,0,str);TextHang(r+5,y/2,0,"#ifr#sds#t");TextHang(-r,y+y,0,"Sun diameter");
}#v07=?>A#t
```

5. Earth's central state and space debris distribution

Appling the acceleration-roll wave to the Moon, as illustrated in Fig.6(a), the Moon has been assigned a quantum number of n=2 in the author's early study [28]. According to the quantum condition, the ultimate acceleration is fitted out to be β=1.377075e+14 (m/s^2) in the earth system. Another consideration is to take the quasi-satellite's perigee into account, for the moon and 2004_GU9 etc., as shown in Fig.6(b), but this consideration requires further understanding of its five quasi-satellites [28].

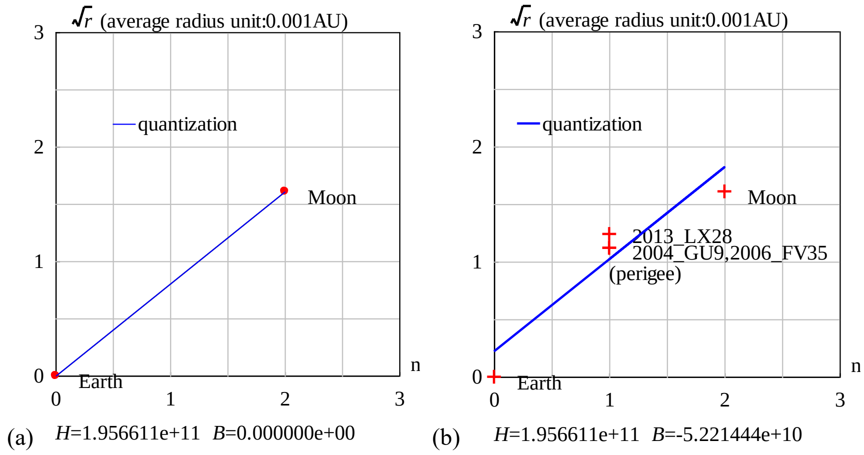

Fig.6 Orbital quantization for moon and quasi-satellites to the Earth, H=hM.

```
<Clet2020 Script>//[26]
char str[200];int i,j,k,N,nP[10]; double x,y,z,M,r_unit,a,b,B,H,r_ave[20],dP[10],D[1000];
double orbit[10]={0,2.57,0,}; double e[10]={0, 0.0549,0,0,0,0,0,0,0,0,};
int qn[10]={0,2,3,4,5,6,7,8,9.,10,}; char Stars[100]={"Earth;Moon;"};
int main(){ N=2; M=5.97237E24; r_unit=1.495978707e8;
for(i=0;i<N;i+=1) {x=orbit[i];y=e[i]; z=x*(1+sqrt(1-y*y))/2;r_ave[i]=z;//average_radius
D[i+i]=qn[i];D[i+i+1]=sqrt(z); }
DataJob("REGRESSION,2",D,dP);b=dP[0];a=dP[1];
SetAxis(X_AXIS,0,0,3,"n;0;1;2;3;");
SetAxis(Y_AXIS,0,0,3," #if#rsr#t (average radius unit:0.001AU);0;1;2;3;");
DrawFrame(0x0166,1,0xafffaf); Polyline(N,D);
SetPen(2,0xff0000); Plot("OVALFILL,0,2,XY,3,3,",D);
for(i=0;i<N;i+=1) {nP[0]=TAKE;nP[1]=i;TextJob(nP,Stars,str);x=qn[i]+0.2;y=sqrt(orbit[i])-0.05;TextHang(x,y,0,str);}
x=GRAVITYC*M*r_unit;z=sqrt(x);H=z*a;B=-z*b;
TextAt(100,450,"#ifH#t=%e   #ifB#t=%e",H,B);
for(i=0;i<N;i+=1) {y=b+a*qn[i];D[i+i]=qn[i];D[i+i+1]=y;}
SetPen(1,0x0000ff);Polyline(N,D,0.5,2.2,"quantization");//check
}}#v07=?>A#t
```

The earth's angular speed is known as ω=2π/(24*3600), unit s^{-1}. Its mass 5.97237e+24(kg), radius 6.371e+6(m), core density 5530(kg/m^3), the ultimate acceleration β=1.377075e+14(m/s^2), the constant hM=1.956611e+11(m^2/s).

We have estimated that the wave overlapping number in the central state of the earth is N=65, the matter distribution $|\psi|^2$ in radius direction is calculated as shown in Fig.7(a), where the self-rotation near its equator has the period of 24 hours:

$$\delta(r)=\frac{1}{hM}\oint_L(v_l)dl=\frac{2\pi r}{hM}\omega r=\frac{2\pi\beta\omega r^2}{c^3}\ . \tag{19}$$

The matter distribution has a central maximum at the earth's heart, which gradually decreases to zero near the earth surface, then rises the secondary peaks and attenuates down off. The radius of the earth is calculated to be r=6.4328e+6 (m) with a relative error of 0.86% using the interference of its acceleration-roll wave. Space debris over the atmosphere has a complicated evolution [7,8], and has itself speed

$$v_l = \sqrt{\frac{GM}{r}}; \quad \delta(r) = \frac{1}{hM}\oint_L (v_l)dl = \frac{\beta}{c^3}\oint_L (v_l)dl = \frac{2\pi\beta}{c^3}\sqrt{GMr} \quad . \tag{20}$$

The secondary peaks over the atmosphere up to 2000km altitude are calculated in Fig.7(b) which agree well with the space debris observations [16]; the peak near 890 km altitude is due principally to the January 2007 intentional destruction of the FengYun-1C weather spacecraft, while the peak centered at approximately 770 km altitude was created by the February 2009 accidental collision of Iridium 33 (active) and Cosmos 2251 (derelict) communication spacecraft [16,18]. The observations based on the incoherent scattering radar EISCAT ESR located at 78°N in Jul. 2006 and in Oct. 2015 [21,22,23] are respectively shown in Fig.7(c) and (d). This prediction of secondary peaks also agrees well with other space debris observations [24,25].

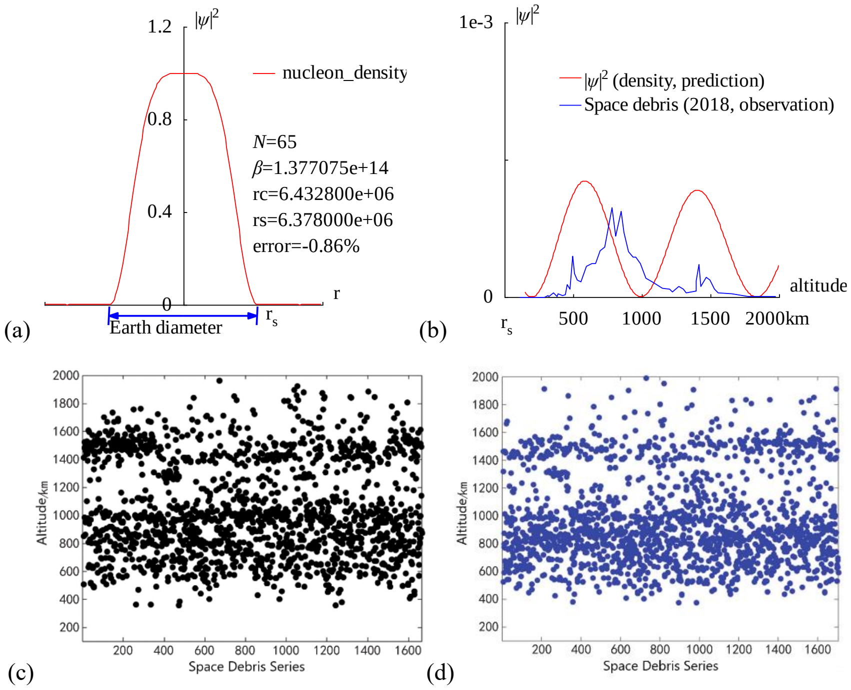

Fig.7 (a) The radius of the Earth is calculated out r=6.4328e+6 (m) with a relative error of 0.86% by the interference of its acceleration-roll wave; (b) The prediction of the space debris distribution up to 2000km altitude; (c) The pace debris distribution in Jul. 2006, Joint observation based on the incoherent scattering radar EISCAT ESR located at 78°N [21]; (d) The space debris distribution in Oct. 2015, Joint observation based on the incoherent scattering radar EISCAT ESR located at 78°N [21].

```
<Clet2020 Script>//[26]
int i,j,k,m,n,N,nP[10]; double H,B,M,v_r,r,AU,r_unit,x,y,z,delta,D[10],S[1000];
double rs,rc,rot,a,b,atm_height,beta; char str[100];
main(){k=80;rs=6.378e6;rc=0;atm_height=1.5e5;n=0; N=65;
beta=1.377075e+14;H=SPEEDC*SPEEDC*SPEEDC/beta;
M=5.97237e24;AU=1.496E11;r_unit=1e-6*AU; rot=2*PI/(24*60*60);//angular speed of the Earth
for(i=-k;i<k;i+=1) {r=abs(i)*r_unit;
if(r<rs+atm_height) v_r=rot*r*r; else v_r=sqrt(GRAVITYC*M*r);//around the Earth
delta=2*PI* v_r/H; y=SumJob("SLIT_ADD,@N,@delta",D); y=y/(N*N);
if(y>1) y=1; S[n]=i;S[n+1]=y; if(i>0 && rc==0 && y<0.001) rc=r;    n+=2;}
SetAxis(X_AXIS,-k,0,k,"r; ; ; ;");SetAxis(Y_AXIS,0,0,1.2,"#if|ψ|#su2#t;0;0.4;0.8;1.2;");
DrawFrame(FRAME_SCALE,1,0xafffaf); x=50;z=100*(rs-rc)/rs;
SetPen(1,0xff0000);Polyline(k+k,S,k/2,1," nucleon_density");
r=rs/r_unit;y=-0.05;D[0]=-r;D[1]=y;D[2]=r;D[3]=y;
SetPen(2,0x0000ff); Draw("ARROW,3,2,XY,10,100,10,10,",D);
Format(str,"#ifN#t=%d#n#ifβ#t=%e#nrc=%e#nrs=%e#nerror=%.2f%",N,beta,rc,rs,z);
TextHang(k/2,0.7,0,str);TextHang(r+5,y/2,0,"r#sds#t");TextHang(-r,y+y,0,"Earth diameter");
}#v07=?>A#t
```

```
<Clet2020 Script>//[26]
int i,j,k,m,n,N,nP[10]; double H,B,M,v_r,r,AU,r_unit,x,y,z,delta,D[10],S[10000];
double rs,rc,rot,a,b,atm_height,p,T,R1,R2,R3; char str[100]; int
Debris[96]={110,0,237,0,287,0,317,2,320,1,357,5,380,1,387,4,420,2,440,3,454,14,474,9,497,45,507,26,527,19,557,17,597,34,63
4,37,664,37,697,51,727,55,781,98,808,67,851,94,871,71,901,50,938,44,958,44,991,37,1028,21,1078,17,1148,10,1202,9,1225,6,
1268,12,1302,9,1325,5,1395,7,1395,18,1415,36,1429,12,1469,22,1499,19,1529,9,1559,5,1656,4,1779,1,1976,1,};
main(){k=80;rs=6.378e6;rc=0;atm_height=1.5e5;n=0; N=65;
H=1.956611e11;M=5.97237e24;AU=1.496E11;r_unit=1e4;
rot=2*PI/(24*60*60);//angular speed of the Earth
b=PI/(2*PI*rot*rs*rs/H); R1=rs/r_unit;R2=(rs+atm_height)/r_unit;R3=(rs+2e6)/r_unit;
for(i=R2;i<R3;i+=1) {r=abs(i)*r_unit; delta=2*PI*sqrt(GRAVITYC*M*r)/H;
y=SumJob("SLIT_ADD,@N,@delta",D); y=1e3*y/(N*N);// visualization scale:1000
if(y>1) y=1; S[n]=i;S[n+1]=y;n+=2;}
SetAxis(X_AXIS,R1,R1,R3,"altitude; r#sds#t;500;1000;1500;2000km ;");
SetAxis(Y_AXIS,0,0,1,"#if|ψ|#su2#t;0; ;1e-3;");DrawFrame(FRAME_SCALE,1,0xafffaf); x=R1+(R3-R1)/5;
SetPen(1,0xff0000);Polyline(n/2,S,x,0.8,"#if|ψ|#su2#t (density, prediction)");
for(i=0;i<48;i+=1) {S[i+i]=R1+(R3-R1)*Debris[i+i]/2000; S[i+i+1]=Debris[i+i+1]/300;}
SetPen(1,0x0000ff);Polyline(48,S,x,0.7,"Space debris (2018, observation) "); }#v07=?>A#t
```

6. Sunspot cycle

The **coherence length** of waves is usually mentioned but the **coherence width** of waves is rarely discussed in quantum mechanics, simply because the latter is not a matter for electrons, nucleon, or photos, but it is a matter in astrophysics. The analysis of observation data tells us that on the planetary scale, the coherence width of acceleration roll waves can be extended to 1000 kilometers or more, as illustrated in Fig.8(a), the overlap may even occur in the width direction, thereby bringing new aspects to wave interference.

In the solar convective zone, adjacent convective arrays form a top-layer flow, a middle-layer gas, and a ground-layer flow, similar to the concept of **molecular current** in electromagnetism. Considering one convective ring at the equator as shown in Fig.8(b), there is an apparent velocity difference between the top-layer flow and the middle-layer gas, where their acceleration-roll waves are denoted respectively by

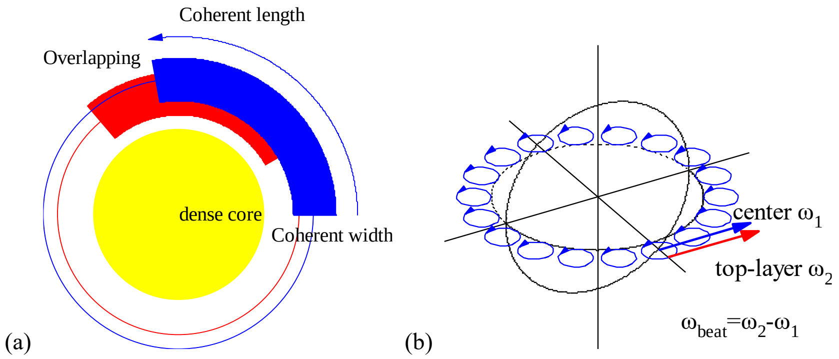

Fig.8 (a) Illustration of overlapping in the coherent width direction. (b) In convective rings at the equator, the speed difference causes a beat frequency.

```
<Clet2020 Script>// [26]
int i, j, k, R,D[500];
main(){DrawFrame(FRAME_NULL,1,0xafffaf);
R=60; SetPen(1,0xffff00);
D[0]=-R; D[1]=-R; D[2]=R; D[3]=R; Draw("ELLIPSE,1,2,XY,0",D);
R=85;    k=15; SetPen(1,0xff0000);
D[0]=-R; D[1]=-R; D[2]=R; D[3]=R; Draw("ELLIPSE,0,2,XY,0",D);
D[0]=0; D[1]=0; D[2]=R-k; D[3]=0; D[4]=R+k;D[5]=0;
Draw("SECTOR,1,3,XY,15,30,130,0",D);
R=95; k=15; SetPen(1,0x00ff);
D[0]=-R; D[1]=-R; D[2]=R; D[3]=R; Draw("ELLIPSE,0,2,XY,0",D);
D[0]=0; D[1]=0; D[2]=R-k; D[3]=0; D[4]=R+k;D[5]=0;
Draw("SECTOR,1,3,XY,15,0,100,0",D);D[4]=R+k+k;
Draw("SECTOR,3,3,XY,15,0,100,0",D);
TextHang(0,0,0,"dense core");TextHang(R-k-k,-k,0,"Coherent width");
TextHang(0,R+k+k+k,0,"Coherent length");TextHang(-R,R+k,0,"Overlapping");
}#v07=?>A#t
```

```
<Clet2020 Script>//Clet is a C compiler[26]
double beta,H,M,N,dP[20],D[2000],r,rs,rot,x,y,v1,v2,K1,K2,T1,T2,T,Lamda,V; int i,j,k;
int main(){beta=2.961520e10; H=SPEEDC*SPEEDC*SPEEDC/beta;
M=1.9891E30; rs=6.95e8;rot=2*PI/(25.05*24*3600);v1=rot*rs;K1=v1*v1/2;//T1=2*PI*H/K1;
v2=0.7346*sqrt(BOLTZMANN*5700/MP)+0.2485*sqrt(BOLTZMANN*5700/(MP+MP));
K2=v2*v2/2;T2=2*PI*H/(K2-K1);T=T2/24*3600*365.2422;
Lamda=2*PI*H/(v2-v1);V=Lamda/T2;
SetViewAngle("temp0,theta60,phi-60");
DrawFrame(FRAME_LINE,1,0xafffaf);Overlook("2,1,60", D);
//TextAt(10,10,"v1=%d, v2=%d, T=%.2f y, λ=%e, V=%d",v1,v2,T, Lamda,V);
SetPen(1,0x4f4fff); for(i=0;i<18;i+=1) {v1=i*2*PI/18; x=70*cos(v1);y=70*sin(v1);Ring();}
SetPen(2,0xff0000);Draw("ARROW,0,2,XYZ,15","80,0,0,80,60,0");
TextHang(100,20,0,"top-layer ω#sd2#t"); SetPen(2,0x0000ff);
Draw("ARROW,0,2,XYZ,15","70,0,0,70,60,0");
TextHang(50,60,0,"center ω#sd1#t");TextHang(140,-30,0," ω#sdbeat#t=ω#sd2#t-ω#sd1#t");
}
Ring(){ k=0;N=20; r=10;
for(j=0;j<N+2;j+=1) {k=j+j+j; v2=j*2*PI/N;
D[k]=x+r*cos(v2);D[k+1]=y+r*sin(v2); D[k+2]=0;}
Plot("POLYLINE,4,22,XYZ,8",D);}
#v07=?>A#t
```

$$
\begin{aligned}
&\psi = \psi_{top} + C\psi_{middle} \\
&\psi_{top} = \exp[\frac{i\beta}{c^3}\int_L (v_1 dl + \frac{-c^2}{\sqrt{1-v_1^{\,2}/c^2}}dt)] \\
&\psi_{middle} = \exp[\frac{i\beta}{c^3}\int_L (v_2 dl + \frac{-c^2}{\sqrt{1-v_2^{\,2}/c^2}}dt)]
\end{aligned} \quad . \tag{21}
$$

Their interference in the coherent width direction leads to a beat phenomenon

$$
\begin{aligned}
&|\psi|^2 = |\psi_{top} + C\psi_{middle}|^2 = 1 + C^2 + 2C\cos[\frac{2\pi}{\lambda_{beat}}\int_L dl - \frac{2\pi}{T_{beat}}t] \\
&\frac{2\pi}{T_{beat}} = \frac{\beta}{c^3}(\frac{c^2}{\sqrt{1-v_1^{\,2}/c^2}} - \frac{c^2}{\sqrt{1-v_2^{\,2}/c^2}}) \simeq \frac{\beta}{c^3}(\frac{v_1^{\,2}}{2} - \frac{v_2^{\,2}}{2}) \\
&\frac{2\pi}{\lambda_{beat}} = \frac{\beta}{c^3}(v_1 - v_2); \quad V = \frac{\lambda_{beat}}{T_{beat}} = \frac{1}{2}(v_1 + v_2)
\end{aligned} \quad . \tag{22}
$$

Their speeds are calculated by

$$
\begin{aligned}
&v_1 \approx 6200\,(m/s) \quad (\approx \text{observed in Evershed flow}) \\
&v_2 = \omega r_{middle} = 2017\,(m/s) \quad (\text{solar rotation});
\end{aligned} \quad . \tag{23}
$$

Where, regarding Evershed flow as the eruption of the top-layer flow, about 6km/s speed was reported [31]. Alternatively, the top-layer speed v_1 also can be calculated by thermodynamics, to be v_1=6244 (m/s) [28]. Thus, their beat period T_{beat} is calculated to be a very remarkable value of 10.38 (years), in agreement with the sunspot cycle value (say, mean 11 years).

$$
T_{beat} \simeq \frac{4\pi c^3}{\beta\left(v_1^{\,2} - v_2^{\,2}\right)} = 10.38\,(years) \ . \tag{24}
$$

The relative error to the mean 11 years is 5.6% for the beat period calculation using the acceleration-roll waves. This beat phenomenon turns out to be a nucleon density oscillation that undergoes to drive the sunspot cycle evolution. The beat wavelength λ_{beat} is too long to observe, only the beat period is easy to be observed. As shown in Fig.9, on the solar surface, the equatorial circumference $2\pi r$ only occupies a little part of the beat wavelength, what we see is the expansion and contraction of the nucleon density.

$$\frac{2\pi r}{\lambda_{beat}} = 0.0032 \quad . \tag{25}$$

This nucleon density oscillation is understood as a new type of nuclear reaction on an astronomic scale.

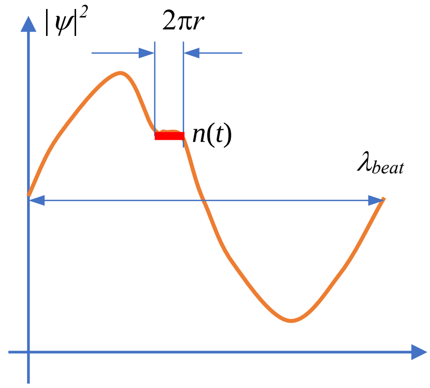

Fig.9 The equatorial circumference 2πr only occupies a little part of the beat wavelength, what we see is the expansion and contraction of the nucleon density.

In the above calculation, although this seems to be a rough model, there is an obvious correlation between solar radius, solar rotation, solar density, ultimate acceleration, and Planck-constant-like constant h.

7. Space debris of neutron stars

Consider a neutron star in its central state with a quantum number n=0, the overlapped wave is given by

$$\begin{aligned} \psi(r) &= 1 + e^{i\delta} + e^{i2\delta} + ... + e^{i(N-1)\delta} = \frac{1-\exp(iN\delta)}{1-\exp(i\delta)} \\ \delta(r) &= \frac{1}{hM}\oint_L (v_l)dl = \frac{2\pi\omega r^2}{hM} = \frac{2\pi\beta\omega r^2}{c^3} \end{aligned} \quad . \tag{26}$$

where N is the overlapping number which is determined by the coherent length of the acceleration-roll wave, δ is the phase difference after one orbital motion, ω is the angular speed of the neutron star rotation. The nucleon density $|\psi|^2$ is illustrated in Fig.10, the core is surrounded by many rings that consists of numerous space debris.

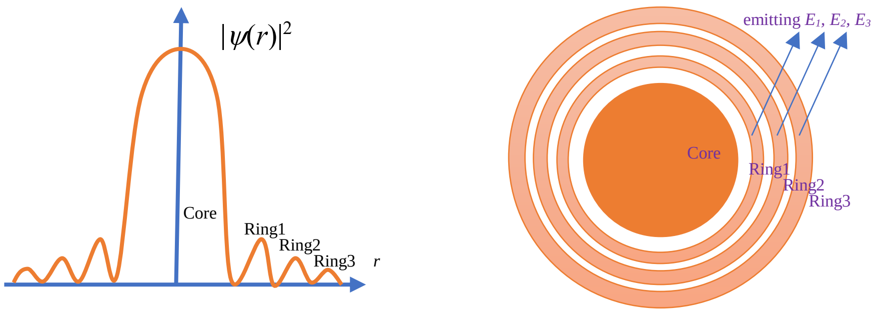

Fig.10 Illustration of the nucleon density $|\psi|^2$, the core is surrounded by many rings.

The acceleration-roll wave of the core's shell has a coherent width which covers all the rings, then a space debris ring has a beat phenomenon which is given by

$$\begin{aligned}&\psi=\psi_{ring}+C\psi_{shell}\\&\psi_{ring}=\exp[\frac{i\beta}{c^3}\int_L(v_1dl+\frac{-c^2}{\sqrt{1-{v_1}^2/c^2}}dt)]\\&\psi_{shell}=\exp[\frac{i\beta}{c^3}\int_L(v_2dl+\frac{-c^2}{\sqrt{1-{v_2}^2/c^2}}dt)]\end{aligned} \quad . \tag{27}$$

Where, the v_1 represents the space debris speed of the ring, the v_2 the neutron star's speed at the equator, they are

$$v_1=\sqrt{GM/r};\quad v_2=\omega r_{equaror} \quad . \tag{28}$$

The coupling constant C determines the strength of the beat phenomenon among the ring due to the interference between the ring and the dense core's rotation. The nucleon density $|\psi|^2$ shows an oscillation in the ring, which turns out to be an expansion and contraction of the neutron particle density in the ring with a beat period

$$\begin{aligned}&\frac{2\pi}{T_{beat}}=\frac{\beta}{c^3}(\frac{c^2}{\sqrt{1-{v_1}^2/c^2}}-\frac{c^2}{\sqrt{1-{v_2}^2/c^2}})\\&|\psi|^2=|\psi_{ring}+C\psi_{shell}|^2=1+C^2+2C\cos[\frac{2\pi}{\lambda_{beat}}\int_L dl-\frac{2\pi}{T_{beat}}t]\end{aligned} \quad . \tag{29}$$

Since every neutron has a magnetic moment μ_n, which has already aligned by the core's polar magnetic field, the expansion and contraction of the ring will cause the electromagnetic field in the ring to vary. Consider an area S perpendicular to neutron's magnetic moments μ_n in the ring. An alternating electric field **E** around the area S is generated by Faraday law:

$$\oint_S \mathbf{E}\cdot d\mathbf{l}=-\frac{d(|\psi|^2\gamma\mu_n S)}{dt}\propto\sin(\frac{2\pi}{T_{beat}}t) \quad . \tag{30}$$

It emits an electromagnetic wave to the sky. All the rings together emit a pulsar that is

$$E=A_1\sin(\frac{2\pi}{T_{beat1}}t)+A_2\sin(\frac{2\pi}{T_{beat2}}t)+A_3\sin(\frac{2\pi}{T_{beat3}}t)+\ldots \quad . \tag{31}$$

Where, A represents amplitude of each wavelet. In space debris, because every neutron magnetic moment has already aligned by the core's polar magnetic field, the alternating electric field **E** is also aligned, therefore pulsar radio signals are often highly linearly polarized. There are three approaches to calculate the pulsar.

(1) Fabry-Perot interference formula

Approximately, suppose every ring emits the same amplitude A, the successive rings have the same phase difference δ, then the pulsar with N ring emissions is simplified by

$$E = A\sin(2\pi\nu_{beat1}t) + A\sin(2\pi\nu_{beat1}t-\delta) + A\sin(2\pi\nu_{beat1}t-2\delta) + \ldots \quad . \tag{32}$$

$$E^2 = A^2\left|\frac{\sin(N\delta/2)}{\sin(\delta/2)}\right|^2 ; \quad \delta \simeq 2\pi\Delta\nu t \quad . \tag{33}$$

Where, $\Delta\nu$ denotes the frequency difference between successive rings. This formula gives out a correct profile of a pulsar from neutron star at first glance, as shown in Fig.11, where the maximal peaks have been truncated.

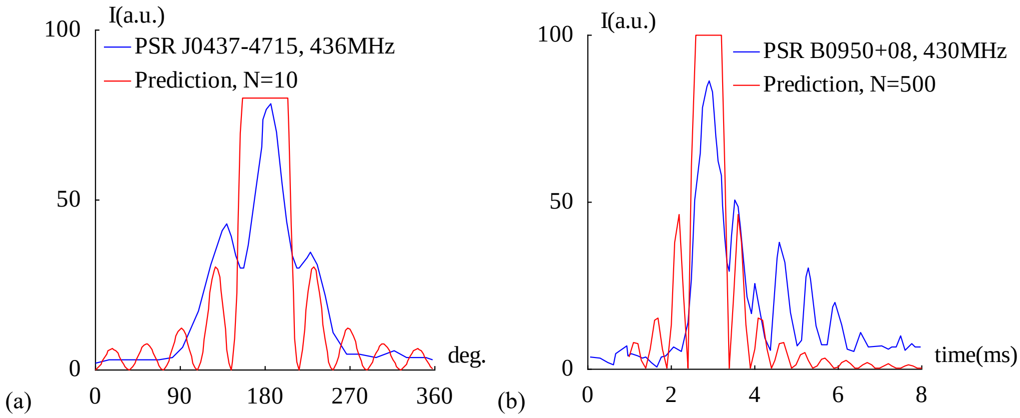

Fig.11 The simulation of pulsar microstructure, (a) PSR J0437-4715, 436Mhz; (b) PSR B0950+08, 430Mhz.

```
<Clet2020 Script>//[26]
int i,j,k,m,N; double x,y,z,D[500],S[500];
double
D_Page217[80]={0.00,1.82,14.96,2.73,30.86,2.73,44.88,2.73,68.26,2.73,82.29,3.64,93.51,6.36,109.40,17.27,123.43,30.91,135.5
8,40.91,139.32,42.73,144.00,39.09,149.61,33.64,154.29,30.00,158.03,30.00,162.70,36.36,171.12,53.64,176.73,65.45,178.60,73.
64,182.34,76.36,186.08,78.18,192.62,70.00,199.17,54.55,203.84,43.64,209.45,33.64,214.13,30.00,216.94,30.00,225.35,32.73,22
9.09,34.55,235.64,30.91,244.05,21.82,252.47,10.91,260.88,7.27,266.49,4.55,280.52,4.55,298.29,3.64,317.92,5.45,331.01,3.64,3
51.58,3.64,358.13,2.73,};
main(){
SetAxis(X_AXIS,0,0,360,"deg.;0;90;180;270;360;");
SetAxis(Y_AXIS,0,0,100,"I(a.u.);0;50;100;");
DrawFrame(FRAME_SCALE,1,0xafffaf);
j=40; SetPen(1,0xff); Polyline(j,D_Page217,10,95,"PSR J0437-4715, 436MHz");
j=180;N=10;i=0;
for(i=0;i<j;i+=1){ z=PI+i*2*PI/j; z/=2; if(z>0) y=sin(N*z)/sin(z); else y=N;
y/=N; y=600*y*y; if(y>80) y=80;    D[i+i]=i+i; D[i+i+1]=y;}
SetPen(1,0xff0000); Polyline(j,D,10,85,"Prediction, N=10");
}#v07=?>A#t

<Clet2020 Script>//[26]
int i,j,k,m,N; double x,y,z,D[500],S[500];
double
D_Page243[142]={0.06,3.58,0.30,3.23,0.48,1.79,0.62,1.08,0.68,4.66,0.94,6.81,0.98,3.94,1.06,4.66,1.20,3.94,1.32,3.23,1.40,3.58,
1.54,1.79,1.66,0.36,1.76,3.58,1.88,3.94,2.06,6.45,2.26,5.02,2.42,13.98,2.48,26.88,2.58,50.54,2.70,64.52,2.76,78.14,2.86,84.59,2.
92,86.02,3.00,82.80,3.06,74.19,3.08,69.53,3.10,66.31,3.14,62.01,3.20,57.71,3.24,48.75,3.28,39.07,3.34,31.90,3.40,29.03,3.46,39
.43,3.54,50.54,3.62,48.39,3.66,42.65,3.82,21.51,3.92,16.49,4.02,25.45,4.26,9.32,4.38,5.38,4.54,33.33,4.60,37.99,4.72,31.90,4.86
,16.85,5.02,6.81,5.14,8.60,5.24,27.60,5.30,30.11,5.34,26.88,5.48,12.90,5.60,7.17,5.74,7.17,5.88,18.64,5.92,19.71,6.08,13.26,6.2
2,5.73,6.38,5.02,6.54,10.75,6.74,6.45,7.04,6.81,7.22,5.73,7.30,6.45,7.40,6.45,7.50,9.68,7.62,5.38,7.78,7.53,7.84,6.45,7.98,6.45,}
;
main(){
SetAxis(X_AXIS,0,0,8,"time(ms);0;2;4;6;8;");
SetAxis(Y_AXIS,0,0,100,"I(a.u.);0;50;100;");
DrawFrame(FRAME_SCALE,1,0xafffaf);
j=71; SetPen(1,0xff); Polyline(j,D_Page243,3.5,95,"PSR B0950+08, 430MHz");
```

```
i=0; N=500; z=1.28*PI;
for(x=1;x<8;x+=0.1){ z=2*PI*(x-2.9)/253; z/=2; if(x>0) y=sin(N*z)/sin(z); else y=N;
y/=N; y=1000*y*y;    if(y>100) y=100;    D[i+i]=x; D[i+i+1]=y; i+=1;}
SetPen(1,0xff0000); Polyline(i,D,3.5,85,"Prediction, N=500");
}#v07=?>A#t
```

If you are not satisfied with the accuracy of this method, refer to the next approach.

(2) Visualization of Riemann's hypothesis [28]

Apparently, each ring emits an amplitude, the phase difference δ between successive rings is also varying. In practice, the pulsar consists of a series of attenuating wavelets with smaller phase differences, may be given by

$$E=\sum_{n=1}^{N}\frac{1}{n^{a}}e^{-i\omega t-ikt\ln n}=\sum_{n=1}^{N}\frac{1}{n^{a}}e^{-i\omega t-ib\ln n};\quad b=kt\ . \tag{34}$$

Where a and k are two experimental constants depicting the amplitude attenuation and phase variation, by re-arranging these symbols, we find that.

$$\begin{aligned}&E=e^{-i\omega t}\sum_{n=1}^{N}\frac{1}{n^{(a+ib)}}=e^{-i\omega t}\zeta(s);\quad s=a+ib=a+ikt\\&|E|^{2}=|\zeta(s)|^{2}\end{aligned}\ . \tag{35}$$

When $N=\infty$, this is the physical picture of the famous zeta function in terms of optics. Defining $x=\ln(n)$, when $n=1$, we get $x=0$; to note that

$$dn=d(e^{x})=e^{x}dx \tag{36}$$

The zeta function can be written as

$$\begin{aligned}&\zeta(s,N)=\sum_{n=1}^{N}e^{-x(a+ib)}\approx\int_{0}^{\ln N}e^{-x(a+ib)}(e^{x})dx=\int_{0}^{\ln N}e^{(1-a-ib)x}dx\\&\zeta(s)=\zeta(s,N)|_{N=\infty}\end{aligned} \tag{37}$$

Obviously, some error has involved for the first several terms, at a later moment, improvement will be made to fix the error.

$$\begin{aligned}&\zeta(s,N)=\sum_{n=1}^{N}e^{-x(a+ib)}\approx\int_{0}^{\ln N}e^{-x(a+ib)}(e^{x})dx=\int_{0}^{\ln N}e^{(1-a-ib)x}dx\\&=\frac{1}{1-a-ib}e^{(1-a-ib)x}|_{x=0}^{x=\ln N}\\&=\frac{1}{1-a-ib}[e^{(1-a)x}\cos(-bx)+ie^{(1-a)x}\sin(-bx)]|_{x=0}^{x=\ln N}\\&=\frac{e^{(1-a)\ln N}\cos(b\ln N)-1}{1-a-ib}+i\frac{-e^{(1-a)\ln N}\sin(b\ln N)}{1-a-ib}\end{aligned} \tag{38}$$

Due to these sin and cos terms, ones have seen obvious oscillations of the zeta function at infinity domain where $\zeta(s,N)$ produces many zeros. This is

$$\begin{aligned}&\zeta(s,N)=\frac{1}{(1-a)^{2}+b^{2}}\{(1-a)[e^{(1-a)\ln N}\cos(b\ln N)-1]\\&+be^{(1-a)\ln N}\sin(b\ln N)\}\\&+i\frac{1}{(1-a)^{2}+b^{2}}\{b[e^{(1-a)\ln N}\cos(b\ln N)-1]\\&-(1-a)e^{(1-a)\ln N}\sin(b\ln N)\}\end{aligned} \tag{39}$$

When the real part and the imaginary part of the zeta function both go to zero, then $\zeta(s)$ equals to zero, they need

$$\begin{aligned}(1-a)[e^{(1-a)\ln N}\cos(b\ln N)-1]+be^{(1-a)\ln N}\sin(b\ln N)=0\\ b[e^{(1-a)\ln N}\cos(b\ln N)-1]-(1-a)e^{(1-a)\ln N}\sin(b\ln N)=0\end{aligned} \tag{40}$$

It is easy to find the zeros of $\zeta(s,N)$ function at

$$\begin{aligned}&\sin(b\ln N)=0, e^{(1-a)\ln N}\cos(b\ln N)=1\\ &\to \quad a=1, b=\pm\frac{j2\pi}{\ln N}, \quad j=0,1,2,3,\ldots\end{aligned} \tag{41}$$

For example, the N rings whose wavelets overlap on the viewing screen under the rule of $\zeta(s,N)$, then $x=ln(N)$; the zeros of zeta function correspond to the minima of light intensity on the view screen. Actually, after improvement on the first several terms in the zeta function, a should be less than 1. All zeros indeed fall on the straight-line $s=a+ib$ in the complex space as the Reimann's hypothesis expects. This is an issue of visualization of Reimann' hypothesis that was discussed in Ref. [28].

(3) Numerical calculation

Computer can be employed to carry out calculation of any type of pulsars, for any purpose.

In this model, the star's core rotates slowly, while the space debris in rings has a very high speed close to the speed of light c, this pulsar electromagnetic radiation has the relativistic period T_{pulse} that is estimated from the first ring by

$$\begin{aligned}&T_{pluse}=\frac{2\pi c^3}{\beta}/(\frac{c^2}{\sqrt{1-v_1^2/c^2}}-\frac{c^2}{\sqrt{1-v_2^2/c^2}})\simeq\frac{2\pi c}{\beta}\sqrt{1-v_1^2/c^2};\\ &\beta=\frac{c^3}{hM}\end{aligned} \tag{42}$$

where h denotes the Planck-constant-like constant with a value of 3.51e-16 $m^2s^{-1}kg^{-1}$, and M denotes the mass of the neutron star. By ignoring the v/c factor under non-relativistic condition, we estimate the periods for various stars as followings

$$\begin{aligned}&M=100M_\odot;\quad T_{pulse}=2.09s\\ &M=10M_\odot;\quad T_{pulse}=0.2s\\ &M=M_\odot;\quad T_{pulse}=20ms\\ &M=0.1M_\odot;\quad T_{pulse}=2.09ms\end{aligned} \tag{43}$$

```
<Clet2020 Script>//[26]
double beta,h,H,M,rs,T;char str[200];
int main(){h=1.51e-16; M=1.9891E30; beta=SPEEDC*SPEEDC*SPEEDC/(h*M);
T=2*PI*SPEEDC/beta; Format(str,"T=%f s",T); TextAt(100,100,str);
} #v07=?>A#t
```

In fact, the space debris in a ring has a very high speed, which cannot be neglected, thus the final pulsar period will be inevitably determined by the v/c factor.

Three distinct classes of pulsars are currently known to astronomers, according to the source of the power of the electromagnetic radiation: (1) rotation-powered pulsars, where the loss of rotational energy of the star provides the power; (2) accretion-powered pulsars (accounting for most but not all X-ray pulsars), where the gravitational potential energy of accreted matter is the power source (producing X-rays that are observable from the Earth); (3) magnetars, where the decay of an extremely strong magnetic field provides the electromagnetic power. Although all three classes of objects are neutron stars, their observable behavior and the underlying physics are quite different [39]. Arming with the acceleration-roll wave and the Planck-constant-like constant, all imaginary spins of neutron stars are not true, instead, neutron star's rings rotate at high speeds.

8. Conclusions

In analogy with the ultimate speed c, there is an ultimate acceleration β, nobody's acceleration can exceed this limit β, in the solar system, β=2.961520e+10(m/s^2). Because this ultimate acceleration is large, any effect related to β will become easy to test, including quantum gravity tests. In this paper, an approach is put forward to connect the ultimate acceleration with quantum theory, as an application, the sunspot cycle is calculated to be 10.38 years due to the ultimate acceleration. The same approach is applied to pulsar microstructure problems. The microstructures of pulsar PSR J0437-4715 at 436Mhz and PSR B0950+08 at 430Mhz are investigated, the calculation results agree well with the observations. Under non-relativistic condition, the pulsar with 100 times solar mass has a period of 2.09s; the pulsar with 10 solar times mass has a period of 0.2s; the pulsar with solar mass has a period of 20ms; the pulsar with a tenth solar mass has a period of 2ms.

References

[1]C. Marletto, and V. Vedral, Gravitationally Induced Entanglement between Two Massive Particles is Sufficient Evidence of Quantum Effects in Gravity, Phys. Rev. Lett., 119, 240402 (2017)

[2]T. Guerreiro, Quantum effects in gravity waves, Classical and Quantum Gravity, 37 (2020) 155001 (13pp).

[3]S. Carlip, D. Chiou, W. Ni, R. Woodard, Quantum Gravity: A Brief History of Ideas and Some Prospects, International Journal of Modern Physics D, V,24,14,2015,1530028. DOI:10.1142/S0218271815300281.

[4]de Broglie, L., CRAS,175(1922):811-813, translated in 2012 by H. C. Shen in Selected works of de Broglie.

[5]de Broglie, Waves and quanta, Nature, 112, 2815(1923): 540.

[6]de Broglie, Recherches sur la théorie des Quanta, translated in 2004 by A. F. Kracklauer as De Broglie, Louis, On the Theory of Quanta. 1925.

[7]NASA, https://solarscience.msfc.nasa.gov/interior.shtml.

[8]NASA, https://nssdc.gsfc.nasa.gov/planetary/factsheet/marsfact.html.

[9]B. Ryden Introduction to Cosmology, Cambridge University Press, 2019, 2nd edition.

[10]D. Valencia, D. D. Sasselov,R. J. O'Connell, Radius and structure models of the first super-earth planet, The Astrophysical Journal, 656:545-551, 2007, February 10.

[11]D. Valencia, D. D. Sasselov,R. J. O'Connell, Detailed models of super-earths: how well can we infer bulk properties? The Astrophysical Journal, 665:1413–1420, 2007 August 20.

[12]T. Guillot, A. P. Showman, Evolution of "51Pegasusb-like" planets, Astronomy & Astrophysics,2002, 385,156-165, DOI: 10.1051/0004-6361:20011624

[13]T. Guillot, A. P. Showman, Atmospheric circulation and tides of "51Pegasusb-like" planets, Astronomy & Astrophysics,2002, 385,166-180, DOI: 10.1051/0004-6361:20020101

[14]L.N. Fletcher,Y.Kaspi,T. Guillot, A.P. Showman, How Well Do We Understand the Belt/Zone Circulation of Giant Planet Atmospheres? Space Sci Rev, 2020,216:30. https://doi.org/10.1007/s11214-019-0631-9

[15]Y. Kaspi, E. Galanti, A.P. Showman, D. J. Stevenson, T. Guillot, L. Iess, S.J. Bolton, Comparison of the Deep Atmospheric Dynamics of Jupiter and Saturn in Light of the Juno and Cassini Gravity Measurements,Space Sci Rev, 2020, 216:84. https://doi.org/10.1007/s11214-020-00705-7

[16]Orbital Debris Program Office, HISTORY OF ON-ORBIT SATELLITE FRAGMENTATIONS, National Aeronautics and Space Administration, 2018, 15 th Edition.

[17]M. Mulrooney, The NASA Liquid Mirror Telescope, Orbital Debris Quarterly News, 2007, April,v11i2,

[18]Orbital Debris Program Office, Chinese Anti-satellite Test Creates Most Severe Orbital Debris Cloud in History, Orbital Debris Quarterly News, 2007, April,v11i2,

[19]A. MANIS, M. MATNEY, A.VAVRIN, D. GATES, J. SEAGO, P. ANZ-MEADOR, Comparison of the NASA ORDEM 3.1 and ESA MASTER-8 Models, Orbital Debris Quarterly News, 2021, Sept,v25i3.

[20]D. Wright, Space debris, Physics today,2007,10,35-40.
[21]TANG Zhi-mei, DING Zong-hua, DAI Lian-dong, WU Jian, XU Zheng-wen, "The Statistics Analysis of Space Debris in Beam Parking Model in 78° North Latitude Regions," Space Debris Research, 2017, 17,3, 1-7.
[22]TANG Zhimei DlNG, Zonghua, YANG Song, DAI Liandong, XU Zhengwen, WU Jian The statistics analysis 0f space debris in beam parking model based On the Arctic 500 MHz incoherent scattering radar, CHINESE JOURNAL 0F RADIO SCIENCE, 2018, 25,5, 537-542
[23]TANG Zhimei, DING, Zonghua, DAI Liandong, WU Jian, XU Zhengwen, Comparative analysis of space debris gaze detection based on the two incoherent scattering radars located at 69N and 78N, Chin . J . Space Sci, 2018 38,1, 73-78. DOI:10.11728/cjss2018.01.073
[24]DING Zong-hua, YANG Song, JIANG hai, DAI Lian-dong, TANG Zhi-mei, XU Zheng-wen, WU Jian, The Data Analysis of the Space Debris Observation by the Qujing Incoherent Scatter Radar, Space Debris Research, 2018, 18,1, 12-19.
[25]YANG Song, DING Zonghua, Xu Zhengwe, WU Jian, Statistical analysis on the space posture, distribution, and scattering characteristic of debris by incoherent scattering radar in Qujing, Chinese Journal of Radio science, 2018 33,6 648-654, DOI:10.13443/j.cjors.2017112301
[26]Clet Lab, Clet: a C compiler, https://drive.google.com/file/d/1OjKqANcgZ-9V5
6rgcoMtOu9w4rP49sgN/view?usp=sharing
[27]Huaiyang Cui, Relativistic Matter Wave and Its Explanation to Superconductivity: Based on the Equality Principle, Modern Physics, 10,3(2020)35-52. https://doi.org/10.12677/MP.2020.103005
[28]Huaiyang Cui, Relativistic Matter Wave and Quantum Computer, Amazon Kindle eBook, 2021.
[29]Huaiyang Cui, Evidence of Planck-Constant-Like Constant in Five Planetary Systems and Its Significances, viXra:2204.0133, 2022.
[30]Huaiyang Cui, Approach to enhance quantum gravity effects by ultimate acceleration, viXra:2205.0053, 2022.
[31]N.Cox, Allen's Astrophysical Quantities, Springer-Verlag, 2001, 4th ed..
[32] S. E. Schneider, T. T. Arny, Pathways to Astronomy, McGraw-Hill Education, 2018, 5th ed.
[33] https://en.wikipedia.org/wiki/El_Ni%C3%B1o%E2%80%93Southern_Oscillation
[34] https://en.wikipedia.org/wiki/Atmosphere_of_Earth
[35] WANG Hui, WANG Aimei , LI Wenshan , LUO Jinxin , ZHANG Jianli, ZUO Changsheng, Changes in key indicators of coastal marine climate in China, Marine Science Bulletin, 2021, 23(1):17-34.
[36] Liping Li et al, Introduction to Atmospheric Circulation, 2nd edition, Science Press, 2021,
[37] https://en.wikipedia.org/wiki/Tropical_cyclone
[38] https://en.wikipedia.org/wiki/Tropical_cyclone_basins
[39] https://en.wikipedia.org/wiki/pulsar.
[40] L A. Lyne and F. Graham-Smith, Pulsar Astronomy, Fourth Edition, Cambridge University Press, 2012.